PNAS RESEARCH ARTICLE | EVOLUTION

Evolutionary adaptation under climate change: *Aedes* sp. demonstrates potential to adapt to warming

Lisa I. Couper[a,b,1], Tristram O. Dodge[a], James A. Hemker[a], Bernard Y. Kim[a], Moi Exposito-Alonso[c,d], Rachel B. Brem[e], Erin A. Mordecai[a], and Mark C. Bitter[a]

Affiliations are included on p. 10.

Edited by David Denlinger, The Ohio State University, Columbus, OH; received September 6, 2024; accepted December 16, 2024

Climate warming is expected to shift the distributions of mosquitoes and mosquito-borne diseases, promoting expansions at cool range edges and contractions at warm range edges. However, whether mosquito populations could maintain their warm edges through evolutionary adaptation remains unknown. Here, we investigate the potential for thermal adaptation in *Aedes sierrensis*, a congener of the major disease vector species that experiences large thermal gradients in its native range, by assaying tolerance to prolonged and acute heat exposure, and its genetic basis in a diverse, field-derived population. We found pervasive evidence of heritable genetic variation in mosquito heat tolerance, and phenotypic trade-offs in tolerance to prolonged versus acute heat exposure. Further, we found genomic variation associated with prolonged heat tolerance was clustered in several regions of the genome, suggesting the presence of larger structural variants such as chromosomal inversions. A simple evolutionary model based on our data estimates that the maximum rate of evolutionary adaptation in mosquito heat tolerance will exceed the projected rate of climate warming, implying the potential for mosquitoes to track warming via genetic adaptation.

evolutionary adaptation | climate warming | mosquito | mosquito-borne disease | *Aedes*

Significance

Global change may have profound impacts on the distribution of mosquito-borne diseases, which collectively cause nearly one million deaths each year. Accurately predicting these impacts is critical for disease control preparedness, and will depend, in part, on whether mosquitoes can adapt to warming—a key open question. Using experimental and genomic data from a relative of major vector species that already experiences a wide thermal gradient, we find that natural mosquito populations have high levels of genetically based variation in heat tolerance that could enable adaptation on pace with warming. Incorporating the potential for adaptive responses may therefore be necessary for accurate predictions of mosquito-borne disease distributions under warming, which is critical for preparing mosquito control interventions.

Climate warming is expected to alter the global distributions of mosquitoes that transmit pathogens, disrupting existing vector control measures and changing the landscape of disease risk (1, 2). Thermal limits constrain mosquito species ranges, dictating the suitable temperatures over which they can survive, develop, and reproduce. Consequently, mosquito ranges are predicted to shift with warming, expanding poleward and toward higher altitudes as temperatures become newly suitable at current cool range edges, and contracting at current warm edges as temperatures become newly prohibitive (3–5). For mosquitoes that vector diseases like dengue, malaria, and West Nile virus, which collectively cause nearly one million deaths annually (6), this process is already underway, as warming-related range expansions have been observed for several species of *Anopheles* (7–9), *Aedes* (10–13), and *Culex* (14, 15) mosquitoes. However, most mosquito and vector-borne disease models project that mosquito distributions will also contract at warm edges as temperatures begin to exceed their upper physiological limits. Whether such warming-driven contractions will actually occur, or whether evolutionary adaptation may enable populations to maintain their warm range edges as temperatures increase, is unknown (16–18). Determining thermal adaptive potential for mosquito species will both augment our understanding of species responses to climate change and inform management strategies for controlling disease spread as climate change progresses.

To persist near current warm edges, mosquitoes may need to rapidly adapt to temperatures beyond their current upper thermal limits. Several common properties of mosquitoes suggest that rapid adaptation is feasible, including short generation times, large population sizes, and steep declines in fitness above their thermal optima (reviewed in ref. 17). However, the extent of variation and heritability in heat tolerance—fundamental components of thermal adaptive potential—remain poorly understood for most mosquito species. Several prior studies have found phenotypic variation in heat tolerance for populations of *Aedes* (19), *Anopheles* (20), *Culex* (21–24), and *Wyeomyia* (25) species mosquitoes when assessed under constant temperature exposures in the lab. While this phenotypic variation putatively reflects heritable variation for thermal tolerance as the studies typically controlled for direct environmental effects (i.e., by using common garden experimental designs), the genomic basis and extent of genetic variation in heat tolerance were not directly investigated. Further, while prior studies have investigated mosquito thermal performance for several life history traits (e.g., larval development rates, pupal survival, adult lifespan) (19–21, 23, 26), the extent to which thermal tolerance at juvenile stages is predictive of tolerance at later developmental stages, and whether such cross-stage

Author contributions: L.I.C., E.A.M., and M.C.B. designed research; L.I.C. performed research; L.I.C. and E.A.M. contributed new reagents/analytic tools; L.I.C., T.O.D., J.A.H., B.Y.K., and M.C.B. analyzed data; M.E.-A. and R.B.B. interpreted data and findings; and L.I.C., M.E.-A., R.B.B., E.A.M., and M.C.B. wrote the paper.

The authors declare no competing interest.

This article is a PNAS Direct Submission.

[1]To whom correspondence may be addressed. Email: lcouper@alumni.stanford.edu.

This article contains supporting information online at https://www.pnas.org/lookup/suppl/doi:10.1073/pnas.2418199122/-/DCSupplemental.

Published January 7, 2025.

tolerances are genetically correlated, remains unknown. Finally, several additional studies have found strong direct evidence for heritable variation in response to acute heat shock in adult *Aedes aegypti* (26, 27), but the underlying mechanisms and genetic basis of this variation were not identified.

The pace at which mosquitoes adaptively track warming temperatures may depend on the underlying genetic architecture of thermal tolerance, including the number of independent loci underpinning phenotypic variation in tolerance and the distribution of these loci throughout the genome (28, 29). Across a diverse range of taxa, traits involved in climate adaptation typically exhibit a polygenic basis, whereby hundreds to thousands of genes underpin adaptive phenotypes (30–35). These adaptive loci have often been shown to cluster within chromosomal inversions, a form of structural mutation in which segments of DNA are broken off and become reattached in the reverse orientation. Suppressed recombination within inversion breakpoints can then facilitate the cosegregation of adaptive alleles and augment their spread within populations (36, 37). In *Anopheles* spp., inversions have been found to underscore adaptive traits including desiccation resistance, larval thermal tolerance, insecticide resistance, host preference, and ecotype formation (38–44). Inversions have also been found to be abundant in *A. aegypti,* however, their role in climate adaptation remains largely unknown (45–48). Overall, the underlying genetic architecture of heat tolerance, including the role of chromosomal inversions, remains poorly understood for most mosquito species, hindering efforts to predict the capacity for adaptive evolution on pace with climate warming, and potentially limiting the applicability of mosquito climate response models.

Here, we investigated the potential for evolutionary adaptation in heat tolerance using the western tree hole mosquito, *Aedes sierrensis*, as a focal test species. In addition to being a major pest species and vector of canine heartworm in western North America, as well as a congener of the major human disease vector species (i.e., *A. aegypti* and *Aedes albopictus*), *A. sierrensis* is abundant, distributed across a wide climate gradient (ranging from southern California to British Columbia) (49), and easy to identify, sample, and manipulate in the lab. Leveraging these properties, we sought to answer the following questions: i) How much standing variation in heat tolerance exists in natural mosquito populations? ii) How does prolonged heat exposure at the larval stage impact acute heat tolerance at the adult stage? iii) What is the genetic architecture of these short- and long-term heat tolerance traits? iv) Could standing variation in thermal tolerance enable natural populations to adapt on pace with climate warming, altering projections of future range shifts?

To answer these questions, we conducted a single generation thermal selection experiment in which we reared a genetically diverse starting population, derived from the center of the *A. sierrensis* range, at either high temperatures (30 °C) that approximately capture the upper thermal limits for prolonged larval survival, or control (22 °C) temperatures that approximately capture the maximum temperature experienced by this population during the larval activity season. Using surviving individuals from both temperature treatments, we assayed adult acute heat tolerance using a thermal knockdown assay, and conducted genome-wide association (GWA) analyses of acute and prolonged heat tolerance. We found large phenotypic variation in acute heat tolerance within the study population, and a putative trade-off in heat tolerance to prolonged versus acute exposure, whereby individuals reared under high temperatures during larval development had significantly lower acute heat tolerance as adults compared to individuals reared under control conditions. Our genomic analysis revealed a polygenic architecture of both heat tolerance traits, and a putative role of chromosomal inversions underpinning thermal adaptation within the species. Using parameter estimates derived from our experimental and genomic data, we then estimated that the maximum rate of evolutionary adaptation in larval heat tolerance typically exceeds that of projected climate warming under simplified conditions. This finding suggests that natural populations may harbor the potential to adapt on pace with warming, and that prior climate-based projections that do not incorporate adaptation may underestimate the ranges of mosquitoes and mosquito-borne disease transmission under future climate conditions.

Results

Extent of Variation in Acute Heat Tolerance. Our thermal selection experiment was conducted on a large, diverse starting population of *A. sierrensis* collected from tree hole habitats across Solano County, CA (mean π = 0.0015; see *SI Appendix*, Figs. S1 and S2 and Table S4 for additional population diversity metrics). Specifically, we reared field-collected individuals at common temperatures (22 °C) for two generations, then implemented a selection experiment design in which F_3 larvae were either maintained at control temperatures of 22 °C—approximately the maximum temperature this population currently experiences during the spring when larvae are developing—or high temperatures of 30 °C—approximately the upper thermal limits for prolonged larval survival (19) (n = 790 total control larvae, 1,943 heat-selected larvae; see *SI Appendix*, Table S1 for sample numbers per experimental round). Surviving individuals from both treatments were returned to control conditions (22 °C) at pupation and reared to adulthood. These temperature conditions generated substantial differences in larval survival between treatments: Survival dropped from 57.8% in the control group to 24.2% in the heat-selected group (across all experimental rounds; see *SI Appendix*, Table S1 for rates per round). Although individuals from both groups experienced the same temperature as pupae (22 °C), individuals in the heat-selected group had lower pupal survival rates compared to the control group (74.3% and 93.2% pupal to adult survival, respectively). This resulted in overall survival rates from larvae to adulthood of 18.0% in the heat-selected group and 53.5% in the control group.

Using all individuals that survived to adulthood from either treatment (n = 122 control, 105 heat-selected individuals), we conducted a thermal knockdown assay—the time to loss of motor function in a warm water bath—a frequently used proxy for acute heat tolerance whereby longer knockdown times indicate greater heat tolerance (26, 27, 50, 51). Our results indicate large individual-level variation in acute heat tolerance in both the heat-selected and control populations (Fig. 1), with adults from the control group ranging in knockdown times from 32.7 to 67.6 min (median: 48.8 min) and those from the heat-selected group ranging from 19.8 to 64.8 min (median: 46.2 min) ($t = 2.65$, $P < 0.01$; differences between groups discussed further below). The variance in knockdown times was marginally larger for the heat-selected group (83.8 and 76.9 for males and females, respectively) than for the control group (56.9, 55.7) ($F = 0.071$, control df = 121, heat-selected df = 104, $P = 0.06$ for both sexes combined; $F = 0.68$, control df = 59, heat-selected df = 52, $P = 0.15$ for males only; $F = 0.72$, control df = 61, heat-selected df = 51, $P = 0.23$ for females only).

Impact of Prolonged Larval Heat Exposure on Acute Adult Heat Tolerance. We found that mosquitoes that underwent heat-selection as larvae had significantly shorter knockdown times as adults than the control group (Linear mixed models, t = –2.15,

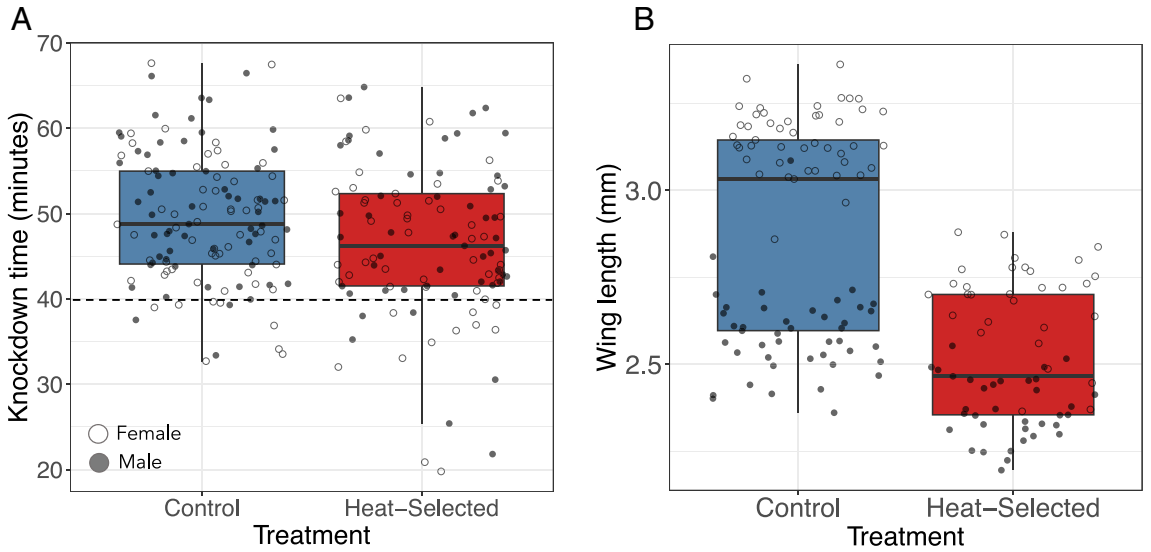

Fig. 1. Acute adult thermal tolerance and wing length are reduced in individuals that experienced larval heat selection. Variation in (*A*) thermal knockdown time (a metric of upper heat tolerance) and (*B*) wing length (a metric of body size) measured in control (blue) and heat-selected (red) *A. sierrensis* adults. Each point denotes the knockdown time or wing length of a single assayed individual. Heat-selected individuals knocked down significantly quicker and had smaller body sizes than control individuals ($P = 0.03$, $P < 0.001$, respectively). Open and filled circles denote females and males, respectively. Points are jittered to aid in visualization. The dashed horizontal line at 40 min on the left plot denotes the time the water bath reached the final set temperature of 38 °C. Points below this line thus denote individuals that knocked down at a lower temperature.

$P = 0.03$; Fig. 1*A*). Specifically, heat-selected larvae knocked down, on average, 3.6 min earlier than control larvae (46.1 ± 8.9, 49.7 ± 7.4 min for heat-selected and control larvae, respectively). To identify proximal mechanisms underlying variation in acute heat tolerance, we measured the wing length—a validated proxy for overall mosquito body size—of each individual used in the thermal knockdown assay (52). We found that adults that underwent heat-selection as larvae had significantly smaller wing lengths (0.31 mm smaller on average) than those from the control group (LMM, t = −16.21, $P < 0.001$, Fig. 1*B*; average wing lengths of 2.51 ± 0.19 and 2.86 ± 0.30 mm for heat-treated and control groups, respectively; *SI Appendix*, Table S2). However, while wing lengths differed between treatment groups, wing length itself was not a significant predictor of knockdown time (LMM, t = −1.17, $P = 0.24$; *SI Appendix*, Table S3). Wing lengths also varied significantly by sex (LMM, t = −22.26, $P < 0.001$, Fig. 1), with the average female wing length being 0.47 mm larger than that of males (2.96 ± 0.25 and 2.49 ± 0.15 mm, respectively; *SI Appendix*, Table S2).

Genomic Architecture of Prolonged and Acute Heat Tolerance. We conducted whole genome sequencing on all 227 *A. sierrensis* individuals that survived to adulthood in the experiment, obtaining an average of 95 million reads and a sequencing depth of ~10× per individual (see *SI Appendix*, Tables S4 and S5 for per-sample summary statistics). We aligned these reads to our de novo *A. sierrensis* reference genome assembly (1.183 Gb; available at DDBJ/ENA/GenBank under the accession JBINJX000000000) and, after quality control and variant filtering, identified 583,889 single nucleotide polymorphisms (SNPs) segregating in our study population. We leveraged these polymorphic sites to identify genomic regions associated with prolonged and acute heat tolerance. For prolonged heat tolerance, we used an F_{st} outlier approach to identify SNPs with elevated differentiation between control and heat-selected groups and, in addition, a case–control GWA between control and heat-selected individuals (*Materials and Methods, Identifying Genetic Variants Associated with Heat Tolerance*). We leveraged the overlap in these approaches to more robustly identify genes underpinning differences in survival between treatments. For acute heat tolerance, we implemented a standard GWA analysis using adult knockdown time as the dependent variable.

We identified hundreds of candidate SNPs associated with thermal tolerance distributed across all three chromosomes. Specifically, we identified 351 and 113 outlier SNPs associated with prolonged larval heat tolerance via the F_{st} outlier ($q < 0.05$ and $F_{st} \geq 0.05$) and case–control GWA [false discovery rate (FDR)-corrected $P < 0.01$), respectively (Fig. 2*A* and *SI Appendix*, Fig. S3). Both approaches produced clusters of significant SNPs in distinct regions of chromosome one, two, and three (Fig. 2*A* and *SI Appendix*, Fig. S3), putatively indicating a set of tightly linked genes, or larger structural variants, driving the signal in these regions (*SI Appendix*, Figs. S5 and S6). The GWA of knockdown time yielded 120 candidate SNPs, but with a much more diffuse distribution across the genome (Fig. 2*B*). As expected, across all candidate SNPs, we quantified systematic allele frequency differences between treatment groups (Fig. 2 *D* and *E*). That is, we found significantly larger differences in candidate SNP frequency between control and heat-selected individuals, or between individuals with high (upper 50% of phenotypic distribution) and low (bottom 50%) knockdown times, relative to a set of matched controls (*Materials and Methods*, *Estimating Allele Frequency Shifts*) (Fig. 2 *D* and *E* and *SI Appendix*, Fig. S4). Together, these findings indicate that heat tolerance—to both prolonged and acute heat stress—results from allele frequency shifts at SNPs located throughout the genome, ultimately suggesting that polygenic adaptation may underpin population persistence under warming.

The large chromosomal regions enriched in SNPs associated with prolonged thermal tolerance (Fig. 2*A*) indicated that larger structural variants, or regions of coadapted gene complexes, may underpin phenotypic variation in this trait. To investigate this, we used genomic data to assess whether chromosomal inversions, which are known to play a pronounced role in climate adaptation in ectotherms including mosquito species (39, 53), segregate in our study population and potentially differentiate individuals based on their thermal tolerance. Using consensus results from four short-read structural variant callers, we identified 89 inversions segregating in our focal populations (after filtering based on

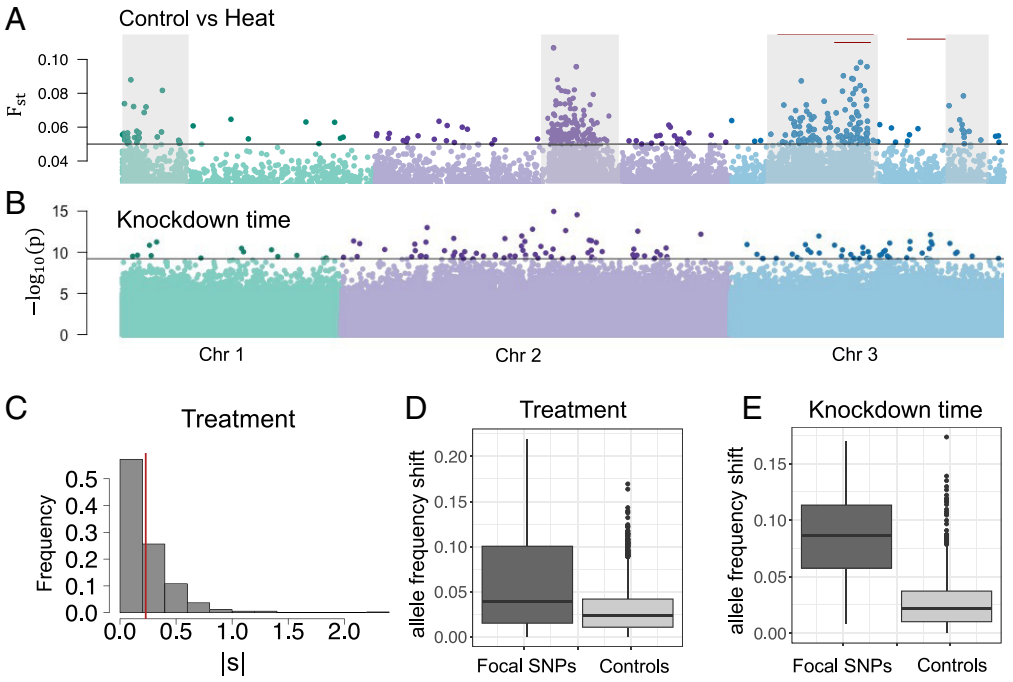

Fig. 2. The genomic architecture of thermal tolerance. (*A*) Genomic position of candidate SNPs significantly associated with larval heat treatment (a measure of prolonged heat tolerance). The black horizontal line indicates the threshold for significance as candidate SNPs (i.e., $q < 0.05$ and $F_{st} > 0.05$). Gray shaded rectangles denote regions with an enrichment of SNPs differentiating treatment groups, relative to the genome-wide average. Red horizontal lines denote the location of chromosomal inversions significantly differentiated in frequency between control and heat-selected larvae. (*B*) Genomic position of candidate SNPs significantly associated with knockdown time (a measure of acute heat tolerance). Here, the black horizontal line indicates the threshold for significance as candidate SNPs based on FDR-corrected $P < 0.001$. (*C*) Distribution of selection coefficients, $|s|$, for candidate SNPs associated with prolonged heat tolerance at the larval stage. The red vertical line denotes the mean. (*D*) Difference in allele frequency distributions for focal SNPs (dark gray) versus their matched controls (light gray) for the larval heat treatment. Here, the focal SNPs from the F_{st} and case–control GWA approaches are shown together. (*E*) Difference in allele frequency distribution for focal SNPs (dark gray) versus their matched control (light gray) for adult thermal knockdown. The black line in each boxplot denotes the median allele frequency difference. See *SI Appendix*, Fig. S4 for allele frequency shifts based on starting minor allele frequency.

size between 1 to 200 Mb and frequency >5%). These were indeed enriched in the specific chromosomal regions where we observed a dramatic elevation in the number of SNPs associated with prolonged, larval heat tolerance (Fig. 2*A* and *SI Appendix, Supplemental Methods*). That is, 62% (n = 55) of the inversions occurred within these regions of interest, which span approximately 31% of the genome. Localized principal components analysis (PCA) on these regions provided further support for the presence of inversions. In particular, within these regions of interest, individuals tended to form three clusters in genomic space, as visualized based on the first two principal component axes—putatively representing standard, inverted, and heterozygous haplotypes—a pattern that was not evident in the PCA on the genome as a whole [*SI Appendix*, Fig. S5; (48)]. We further identified a total of three inversions that were significantly differentiated in frequency between control and heat-selected individuals, two of which fell within these regions of interest (Fig. 2*A* and *SI Appendix*, Fig. S6 and Table S6). We further identified three inversions that were significantly differentiated between individuals from the top 25% and bottom 25% of knockdown times, after controlling for treatment and sex (*SI Appendix*, Table S6). While the patterns observed here, in combination with mounting research in other *Aedes* spp. (39, 54, 55), suggests that inversions may underpin climate adaptation in a range of mosquito species, inferences from short-read sequencing data are limited, and future research leveraging long-read sequencing data to validate and resolve the particular inversions segregating and driving phenotypic differentiation is warranted.

We next generated a list of genes putatively underlying outlier SNP differentiation. Specifically, by identifying all genes within 50 kb of each focal SNP, we identified 293, 105, and 114 annotated genes for the aforementioned three approaches, respectively (i.e., F_{st} and GWA between control and heat-selected individuals, and GWA on knockdown time) out of a total of 30,554 predicted genes across the genome (*SI Appendix*, Fig. S7). We found that the number of overlapping candidate genes identified by the two approaches capturing prolonged heat tolerance (n = 13) was significantly greater than expected by chance (95% CI from expectation: 1.30 to 1.51, $P < 0.01$) (*SI Appendix*, Fig. S7), supporting the robustness of these two methods at capturing similar candidate genes from the same phenotypic data. These overlapping genes mapped to genes previously associated with heat or environmental stress responses in other ectotherm species including histone H3 [involved in heat shock memory (56, 57)], profilin [an actin-binding protein that may function as a molecular chaperone (58, 59)], and cytochrome P450 [involved in thermal stress responses in a wide range of taxa (58–62)] (*SI Appendix*, Table S7). The number of overlapping genes between the prolonged and acute heat tolerance approaches (n = 3, 3) was also significantly greater than expected by chance (95% CI: 1.30 to 1.50, 0.48 to 0.62, $P < 0.01$ for both) (*SI Appendix*, Fig. S7), potentially suggesting shared genetic pathways between prolonged and acute heat tolerance phenotypes.

Investigating Potential to Adapt on Pace with Warming. We investigated whether the level of standing variation in heat tolerance observed here could fuel adaptation on pace with climate warming using a simple evolutionary rescue model parameterized by our experimental data. Specifically, we estimated the maximum rate of evolutionary adaptation in prolonged larval heat tolerance, and compared this to rates of change in mean daily temperature during the larval activity period (typically January – April),

projected under a moderate warming scenario [Representative Concentration Pathway 4.5 (RCP 4.5)]. We focused on larval heat tolerance because our recent investigation of thermal tolerance across life stages in this species indicated that larval survival may be the bottleneck to thermal adaptation (19). We note several simplifying assumptions that may limit the accuracy of our predictions, including the absence of phenotypic plasticity and/or impacts of concurrent abiotic and biotic stressors in the model; the focus on a single trait underlying adaptation (i.e., no constraints or trade-offs); the assumption of constant heritability and phenotypic variance over time and uniform genomic variance across space (i.e., range edge populations are assumed to have similar genetic variation as central populations); and the use of selection strength estimated as the difference in survival between our experimentally imposed temperature treatments (i.e., 30 versus 22 °C), which was guided by, but not specific to, the shift in temperatures that natural populations may experience (*Materials and Methods, Estimating Adaptive Potential*). For these reasons, we use this modeling approach to estimate the potential parameter space of evolutionary adaptation under idealized conditions, rather than to obtain a precise estimate of adaptation expected under natural settings. Using this approach, we found that estimated rates of adaptation exceed rates of warming under most of our experimentally estimated or literature-derived parameter values (Fig. 3 and *SI Appendix*, Fig. S8). Specifically, the maximum estimated rate of evolutionary change derived from our experimental and genomic data (i.e., point estimates for selection strength, heritability, and phenotypic variation) and previously estimated rates of maximum mosquito population growth (r_{max}) ranged from 0.033 to 0.051 °C/y (for r_{max} = 0.15 and 0.35, respectively), exceeding projected rates of warming in mean spring temperatures across the southern portion of the *A. sierrensis* distribution (0.026 °C/y). We consider rates of warming in mean spring temperatures across the southern *A. sierrensis* distribution projected under RCP 4.5 to be the most ecologically relevant metric of warming, but we also consider alternative metrics including the projected rate of change in maximum daily spring temperatures and mean annual temperatures across this same extent under RCP 4.5 (0.040, 0.015 °C/y, respectively), the projected rate of change in annual mean temperatures across the southeastern United States under RCP 4.5 and RCP 8.5 (0.031, 0.035 °C/y, respectively), and recently observed rates of warming in annual mean temperature across North America (0.027 °C/y) (*SI Appendix*, Fig. S8 and Table S9). Across these metrics of warming, our results provide empirical support for the potential for evolutionary adaptation in this population in response to climate warming.

Discussion

Nearly all climate-based projections of future mosquito and mosquito-borne disease distributions assume that mosquitoes will migrate to track their current niches rather than evolve in response to temperature change (17, 26, 63). We examined the potential for thermal adaptation using a selection experiment conducted on the western tree hole mosquito, *A. sierrensis*, a congener of major disease vector species, *A. aegypti,* and *A. albopictus*. Our results suggest that evolutionary adaptation is likely a viable and important component of mosquito responses to climate warming.

Large Within-Population Variation in Acute Heat Tolerance. We found a high level of standing phenotypic variation in heat tolerance within a single, field-derived mosquito population, underpinned by several hundred genes and an abundance of chromosomal inversions. In particular, when exposed to acute high temperature stress, we found that the time to loss of motor function (i.e., "knockdown time") varied from 32.7 to 67.6 min between individuals from a single starting population (here, the control group), despite having experienced the same thermal environment for the prior two generations (i.e., 22 °C). This variation in acute heat tolerance was even larger—ranging from 19.8 to 64.8 min—in individuals that were exposed to prolonged heat stress as larvae (i.e., treatment group, 30 °C). These findings match recent observations of large and heritable variation in acute heat tolerance in related *Aedes* species (26, 27). As genetically based trait variation is critical for adapting to changing conditions (64, 65), our results suggest that *A. sierrensis* may harbor standing variation in heat tolerance that could enable adaptation to aspects of climate warming.

Prolonged Heat Exposure as Larvae Led to Lower Acute Heat Tolerance at the Adult Stage. Our selection experiment also revealed potential costs or trade-offs between prolonged heat exposure during rearing and acute heat tolerance in subsequent life stages. In particular, we found that individuals reared at 30 °C ("heat-selected") as larvae had significantly lower acute heat tolerance as adults (as evidenced by shorter knockdown times) than those reared at 22 °C ("control"). This finding contrasts with prior empirical and theoretical work in thermal biology

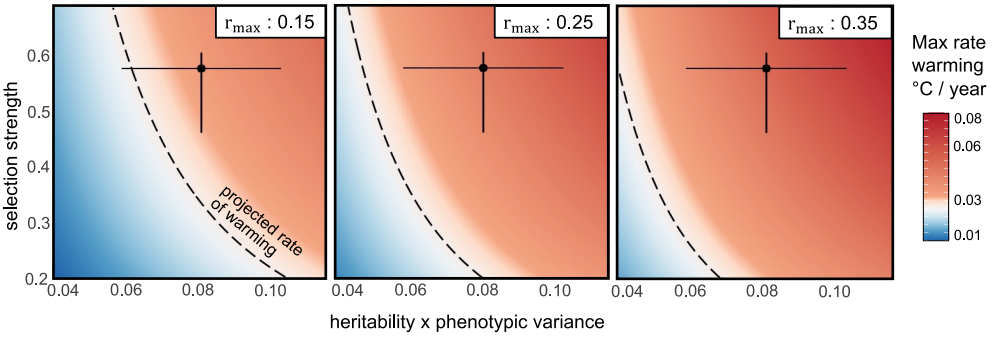

Fig. 3. Rates of evolutionary adaptation typically exceed projected rates of climate warming. Colors denote the maximum rate of warming (°C/y) to which populations could adapt (equivalent to the model-estimated maximum rate of evolutionary change). The *x*-axis denotes potential values for the product of heritability (h^2) and phenotypic variance (σ_p^2), and the *y*-axis denotes potential values for selection strength (γ). The black circle on each plot denotes the point estimate for these three parameter values from our experimental and genomic data and the error bars capture the range of these parameters made under varying model assumptions (*Materials and Methods*, *Estimating Adaptive Potential*). The isolines denote the rates of warming in daily mean temperature during the spring across the southern portion of *A. sierrensis* distribution (0.026 °C/y). Error bars and point estimates to the right of the isolines reflect scenarios under which the population's estimated maximum rate of evolutionary adaptation exceeds the projected rate of warming. The three panels span previously estimated rates of maximum mosquito population growth rates (r_{max} = 0.15, 0.25, and 0.35 for the *Left*, *Center*, and *Right* panels, respectively).

finding that exposure to high temperatures at early life-stages leads to acclimation and higher heat tolerance in adulthood for ectotherms (66–73), including in related *Aedes* species (74). However, our result may be explained by well-supported mechanisms related to variation in adult body size resulting from developmental temperature and/or an accumulation of thermal injury (discussed below).

We found substantial differences in adult body size due to rearing temperature: Individuals reared at 22 °C had approximately 10% larger wing lengths than those reared at 30 °C. Larger adults, in turn, are typically able to endure longer durations of thermal stress due to slower rates of resource depletion and water loss under stress, and higher thermal inertia (38, 75–78). Accordingly, prior studies in ectotherms, including *Aedes*, have found that larger adult body sizes are associated with higher upper thermal limits, as measured by longer knockdown times (52, 77, 79–81). Our results suggest a link between these prior findings, with warmer developmental temperatures leading to smaller adult mosquito body sizes, which may in turn drive the observed reduction in acute heat tolerance (though we note that wing length alone was not a significant predictor of knockdown time in our experiment). However, our findings could also be due to an accumulation of thermal injury, whereby physiological stress incurred during prolonged heat exposure at the juvenile life stage compromises acute responses to thermal stress at the adult life stage. In our experiment, survivorship differed markedly between larval heat treatments, with approximately 18% of heat-selected individuals surviving from larvae to adulthood compared to 54% of control individuals. Although all individuals from both the control and heat-selected group were maintained as pupae and adults at control temperatures (22 and 20 °C, respectively) for several days prior to acute heat tolerance measurements, individuals may have incurred heat damage during the larval stages that was irreparable and/or that required substantial energetic allocation to repair. Differentiating between these potential mechanisms—body size and energetic reserve variation versus thermal injury—which are nonmutually exclusive, will ultimately require rearing individuals across thermal environments for several generations (e.g., ref. 27).

Polygenic Architecture of Prolonged and Acute Heat Tolerance. Our investigation of the genomic architecture of thermal tolerance used a de novo chromosome-level reference genome assembly for *A. sierrensis* (1.183 Gb, available at DDBJ/ENA/GenBank under the accession JBINJX000000000) and revealed a polygenic architecture for both prolonged and acute heat tolerance. That is, we identified hundreds of candidate SNPs distributed across the *A. sierrensis* genome that were associated with surviving prolonged heat exposure or resisting acute thermal stress. These candidate SNPs were identified using both genomic differentiation (F_{ST}) and GWA approaches, and rigorous quality filtering to reduce false positives. These candidate SNPs had significantly larger differences in frequency between groups (i.e., heat-selected versus control individuals or short versus long knockdown times) than control SNPs of similar starting frequency and chromosomal position, strengthening inference of their association with thermal tolerance.

The genomic regions with an elevated signal of SNPs associated with thermal tolerance could indicate regions of selection in which structural genomic changes, such as chromosomal inversions, insertions, deletions, and/or duplications, are present. As inversions have previously been implicated in mosquito climate adaptation and pathogen infection susceptibility (39, 54, 82), we quantified their potential role in the genomic patterns of selection observed in our experiment. We found inversions to be putatively pervasive within the *A. sierrensis* genome: 89 inversions between 1 to 200 Mb in length and at >5% frequency segregated within our focal populations. These were enriched in the specific chromosomal regions where we observed a dramatic elevation in the number of SNPs associated with larval heat tolerance (Fig. 2*A* and *SI Appendix*, Figs. S5 and S6 and *Supplemental Methods*). Further, two inversions within this region exhibited systematic frequency differences between control and heat-selected larvae, suggesting their role in mosquito heat stress responses. This is consistent with a large body of literature, including in *Anopheles* and *Aedes* spp., finding that inversions are an important mechanism of ecological adaptation as suppressed recombination between the inversion breakpoints can lead to coadapted gene complexes and/or preserved combinations of locally adapted alleles (36–44, 83, 84). In particular, the acquisition of inversions *2La* and *2Rb* through introgression from *Anopheles arabiensis* is thought to have enabled *Anopheles gambiae* to expand its ecological niche and become the dominant malaria vector in much of sub-Saharan Africa (40, 41, 85–87). Similarly, several chromosomal inversions in *Anopheles funestus*—an additional key malaria vector in tropical Africa—were found to underscore adaptation to an anthropogenic larval habitat (irrigated rice fields), enabling niche diversification that may challenge vector control efforts (39). In *A. aegypti*, evidence suggests that inversions are present across the three chromosomes, and may be associated with adaptive traits such as host feeding preference (45–48). However, because the short-read sequencing data used in this analysis are limited in their ability to reveal structural variants (though inversions with systematic differences between treatments are unlikely to be technical artifacts), further work using long-read sequencing technology and/or cytogenetic analysis is necessary to resolve the inversions segregating in our focal species and their phenotypic impacts.

Among the candidate thermal tolerance SNPs, several mapped to genes previously associated with responses to heat or other environmental stressors in a range of ectotherms (*SI Appendix*, Table S7). In particular, genes associated with prolonged heat tolerance in our experiment included histone H3, previously implicated in heat shock memory and enhanced survival under subsequent heat exposure (56, 57); profilin, an actin-binding protein that may function as a molecular chaperone and play an important role in the heat stress response (58, 59); and cytochrome P450, a class of proteins implicated in the thermal stress response in plants (60), corals (61), and insects (62). We also identified several genes that were associated with both prolonged and acute heat tolerance, exceeding the expected number of genes that would overlap just by chance (i.e., six observed overlapping genes versus ~2 expected out of a total of 493 candidate genes), suggesting some shared pathways of acute and chronic heat tolerance. These overlapping genes mapped to genes involved in DNA damage repair in ectotherms ("DNA repair endonuclease") (88, 89), and sensory perception in *A. aegypti* ("dopamine receptor-1") (90) or *A. albopictus* ("sensory neuron membrane protein 2") (91). As the candidate genes identified here largely align with prior associations of abiotic stress resistance in other ectotherms, they may be valuable targets for future transcriptomic and functional studies to dissect their role in mosquito heat tolerance.

Potential to Adapt on Pace with Warming. Our data suggest that natural mosquito populations may harbor the potential to adapt on pace with climate warming, and thus incorporating this adaptive potential is critical to accurately projecting the range of mosquitoes under future climates. In particular, we parameterized a simple evolutionary model estimating the maximum potential rate of evolutionary change in larval thermal tolerance in comparison with expected rates of warming during the spring (the larval

activity period). We focused on larval heat tolerance as recent evidence suggests this may be the bottleneck to thermal adaptation in this species (19). We found that, under most parameter values informed by our experimental and genomic data, estimated rates of adaptation exceeded projected rates of warming in mean spring temperatures under a moderate warming scenario (i.e., RCP 4.5). This suggests that the warm edge limits of the species may not contract as quickly as assumed in most models, and the overall suitable range for the species may increase under global warming. Environmental stress responses can vary between congeneric ectotherm species (92, 93), so the extent to which our estimates of heritability and selection strength apply to disease vector species such as *A. aegypti* and *A. albopictus* remains unknown.

Our evolutionary model did not incorporate the presence of daily and seasonal temperature variation, concurrent stressors in other abiotic or biotic factors (*e.g.*, drought, resource availability, land use change, human insecticide applications), or phenotypic plasticity, which may alter rates of adaptive evolution (64, 94–97). In particular, phenotypic plasticity may be a key mechanism of mosquito responses to warming, particularly to short-term thermal extremes (24, 27, 51, 98), and may trade off with basal heat tolerance (99–101). However, the extent of phenotypic plasticity in natural mosquito populations and its relationship to basal thermal tolerance and adaptive potential was not directly explored here and remain poorly understood. Another limitation of this modeling approach is that the strength of selection was simply estimated as the difference in survival between our experimentally imposed temperature treatments. These temperatures—22 and 30 °C—were chosen to approximately capture the current maximum temperature this population may experience during the larval activity period and the upper thermal limits for larval survival, respectively, but are not specific to the projected shift in temperatures that natural populations may experience. Natural populations experience temperature variation on multiple time scales and may experience future warming as gradual, punctuated, and/or accelerating changes in temperature over time, each of which may impose different strengths of selection which could be lesser or greater than our estimate (102–104). Similarly, we assume directional changes in alleles under selection that are consistent over generations and responses to selection that are uniform across space. We do not consider environmental gradients in selection, potentially negative effects of gene flow on adaptive capacity (i.e., "swamping"), or reduced genomic variation in range-edge versus central populations—each of which may alter, and likely reduce, the realized adaptive potential (105, 106). Last, our model considered only evolutionary adaptation in prolonged heat tolerance at the larval stage, which may have ecological trade-offs, and/or a distinct genetic underpinning from other traits enabling heat stress resistance or avoidance such as quiescence. In general, evolutionary models such as that used here have rarely been validated in natural settings, thus we interpret these as results under idealized conditions that warrant further investigation under more ecologically realistic settings.

Despite these caveats, the evidence for climate adaptive potential presented here aligns with several prior studies finding high levels of phenotypic or genomic variation in heat tolerance in natural mosquito populations (26, 27, 41, 107), phenotypic shifts in heat tolerance over time (27), and rapid genomic shifts when invading novel climates (63). Collectively, these findings provide compelling evidence that evolutionary adaptation could enable mosquito populations to persist in regions where they are otherwise expected to decline due to warming. This potential for adaptation to heat tolerance is important in light of projections based on fixed mosquito heat tolerance that predict declines at warm range edges, for example in *A. albopictus*-transmitted arboviruses in the tropics (5) and in *A. gambiae*-transmitted malaria in western Africa (108) in coming decades. Our findings suggest that mosquitoes have currently underrecognized potential for thermal adaptation that may alter mosquito species distributions and disease transmission ranges under climate warming.

Materials and Methods

Source Population. This study was conducted on *A. sierrensis*, a widespread endemic mosquito that inhabits water-filled tree holes in forested habitats across western North America (49). The species life cycle is largely driven by temperature and precipitation with eggs hatching after fall and winter rains, juvenile development occurring throughout the subsequent months, and adults emerging as the tree holes dry out in the spring and summer (see *SI Appendix*, Fig. S12 for temperatures recorded from tree holes near the study region). The species is likely univoltine across its range with an egg stage diapause during the dry season and a fourth instar larval diapause for northern-latitude populations (109).

A. sierrensis used in this study were collected as larvae by Solano County Mosquito Abatement District personnel from various tree holes in Solano County, California in spring, 2019 (Fig. 4 and *SI Appendix*, Fig. S13). Average daily temperatures in this region during the spring (here defined as January – April) are approximately 10 to 15 °C and average daily maximum temperatures are approximately 14 to 22 °C respectively (110). Collected larvae were reared for two generations at 20 to 22 °C at the Solano County Mosquito Abatement District to minimize direct environmental effects on thermal tolerance and maternal/cross-generational effects. Approximately 300 females from the F_2 generation were blood-fed and produced eggs for use in the experiment. Prior to experimentation, eggs were transported to Stanford University and maintained at 20 to 22 °C and 6 h/18 h light/dark cycles to prevent diapause. Our focus on patterns of variation within a single population allowed the identification of trait variation to be minimally impacted by population substructure, which can drive spurious signals in association-based studies (111). We further selected our focal population to be from the center of the species range, and thus most likely harboring mutations present across the range and insensitive to idiosyncratic patterns of diversity that can accumulate at range edges (112).

Selection Experiment Set-Up. The single-generation selection experiment began with *A. sierrensis* at the egg stage (Fig. 4). Egg paper containing approximately 200 eggs each were hatched in plastic trays containing 1L boiled distilled water cooled to room temperature and one tablespoon larval food (four parts high protein cat chow: four parts alfalfa pellets: one part nutritional yeast). All eggs were hatched at 22 °C under 14 h/10 h light/dark cycles. Upon hatching, individual larvae were then designated to either the control or treatment group, which each consisted of four identical replicates (Fig. 4). Individuals were randomly assigned to a replicate such that approximately 30% of larvae were designated to replicates in the control group and 70% to replicates in the treatment (heat-selected) group. This uneven assignment was due to expected reduced survivorship in the heat-selected groups, as observed during pilot experiments, to ensure adequate sample sizes for downstream analyses. Control group individuals were maintained at 22 °C through to adulthood (approximately 18 d after hatching). Treatment group larvae were placed in incubators that were ramped from 25 to 30 °C over the course of 3 d. This ramping period was used because prior pilot experiments in the lab found high larval mortality (>95%) when transferring 1st instar larvae directly from 22 to 30 °C. These specific temperature treatments–22 and 30 °C were specifically chosen to approximate the currently daily maxima for this population in the spring, when larvae are developing, and the upper thermal limits for larval survival as measured under constant temperature conditions (19). To reduce accumulated thermal stress across the lifetime, treatment group larvae that survived to pupation were transferred to the control temperature (22 °C) upon pupation (approximately 14 d after hatching) and remained here through adulthood (approximately 4 d after pupation). Thus, our selection experiment specifically aimed to target prolonged thermal tolerance at the larval stage, leading to genotype frequency differences between the control and heat-selected adults that reflect this early life-history selection event. Individuals from each replicate of the control and treatment groups were maintained in plastic cups and fed one teaspoon larval food every 3 d. Once reaching the adult life stage, individuals

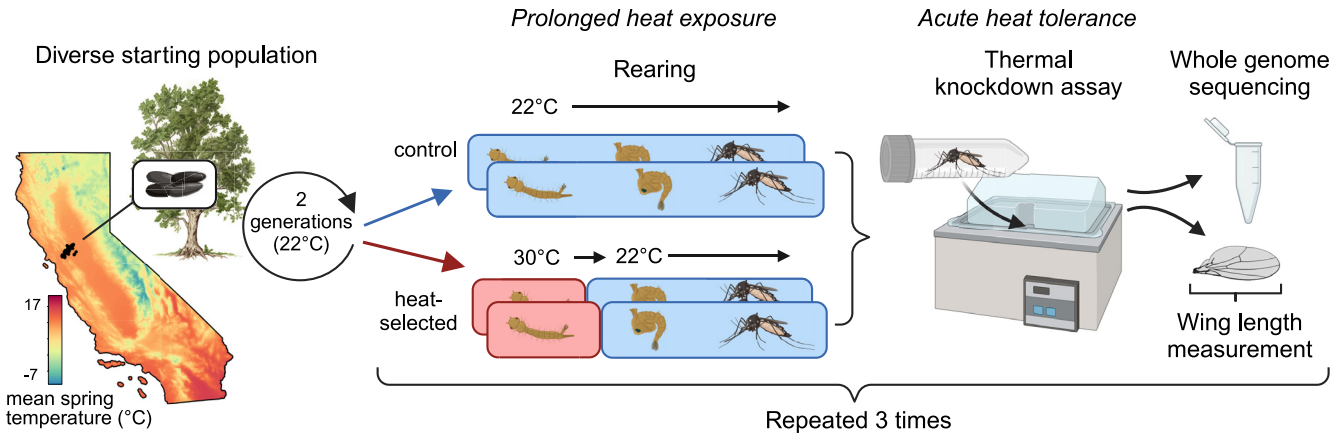

Fig. 4. Assessing chronic and acute heat tolerance in a genetically diverse field-derived population of mosquitoes. A diverse starting population was obtained from tree hole habitats across Solano County, CA, with the original sampling locations denoted on the map. Map colors denote variation in average daily temperatures in the spring—the larval activity period. All individuals were reared under lab conditions for two generations, and the resulting F_3 eggs were used in the experiment. Eggs were hatched at 22 °C, and 24-h larvae were randomly designated into replicated control or heat-selected groups. Individuals were reared at 22 °C (control) or 30 °C (heat-selected) as larvae. All individuals were maintained at 22 °C at the pupal and adult life stages. Acute heat tolerance was assayed via thermal knockdown on individuals 48 to 72 h after eclosion. All individuals were then preserved for DNA sequencing and body size approximation. The full experiment was conducted three times for biological replication.

were transferred to breeding cages (BioQuip). The heat-tolerance assay was performed on adults that had eclosed 48 to 72 h prior and had not been sugar- or blood-fed. This procedure–from hatching to knockdown assay–was conducted three times to ensure our results were robust to minor variation in laboratory experimental conditions.

Heat-Tolerance Assay. We used a thermal knockdown assay to assess the upper heat tolerance of adult *A. sierrensis* from the control and treatment groups. This is a commonly used assay to measure upper thermal limits of arthropods, including mosquitoes, and has been shown to accurately predict insect species distributions in the field and to be a relevant proxy for fitness under heat stress (19, 26, 27, 50, 51, 113) (but we note that methodological details such as the initial and final temperature conditions have varied between studies). We followed the thermal knockdown protocols of refs. 114 and 115. Specifically, adult *A. sierrensis* were placed in individual 5-mL plastic vials and immersed in a water bath set initially to 28 °C. After a 15-min acclimation period, the water bath temperature was increased to 38 °C at a rate of 0.5 °C per minute (116). Heat tolerance was scored as the knockdown time–the time after immersion at which an individual loses muscle function and can no longer right itself from a dorsal position. This assay thus represents the acute thermal tolerance of all control individuals and individuals that had survived prolonged exposure to thermal stress at the larval stage. Immediately after knockdown, samples were placed in individual tubes and stored at −80 °C. Assays were performed on eight adults at a time and the same observer performed all assays.

Body Size Estimates. To estimate the body size of each individual used in the experiment, we measured mosquito wing length–a commonly used proxy, including in *Aedes* spp. mosquitoes (117–122). The wing length-body size relationship has been validated in *A. sierrensis* specifically, and corroborated with measurements of thorax lengths, with no systematic differences identified in wing to thorax length ratios across temperatures (52). Prior to DNA extraction, we detached the left wing using fine forceps, attached it to a microscope calibration slide, and used *ImageJ* (123) to measure the distance from the alula to the wing tip, excluding the wing scales (*SI Appendix*, Fig. S9) (124, 125). We excluded any wings that were damaged during removal or the knockdown assay.

Statistical Analysis on Knockdown Assay. To investigate variation in knockdown times by treatment, we used a linear mixed-effects model implemented using the "lme4" package in R (126). We used knockdown time as the outcome variable and treatment and sex as categorical fixed effects. To account for potential variation between biological replicates (as the experiment was repeated in three rounds) and knockdown assays, we included these as random intercepts in the model.

DNA Extraction and Sequencing. We extracted DNA from each individual using an AllPrep DNA/RNA kit (Qiagen, Valencia, CA) and used approximately 25 ng genomic DNA per sample to prepare libraries using the Illumina DNA prep kit. The libraries were pooled and sequenced as 150-bp paired-end reads on four lanes of a NovaSeq 600 Illumina at the Stanford Genome Sequencing Service Center.

Reference Genome Assembly. We assembled a de novo reference genome for *A. sierrensis* to facilitate genomic analysis in the absence of a previously available reference for this species (available at DDBJ/ENA/GenBank under the accession JBINJX000000000) (*SI Appendix, Supplemental Methods*). Briefly, we selected a single adult female *A. sierrensis* that was field-collected from Eugene, Oregon for PacBio HiFi sequencing. We then assembled the genome using Hifiasm v0.16 with default parameters (Cheng et al. (127)). Evaluating the assembly for missing or duplicated genes indicated a high level of completeness (97.1%) and duplication rates on par with that of recent de novo assemblies in other mosquito species (*SI Appendix, Supplemental Methods*) (128–130). We used the *A. aegypti* Aaeg L5 genome (NCBI BioProject ID: PRJNA940745) to scaffold the draft assembly into chromosomes using RagTag (131), and found that 96% (1.139 Gb) of our assembly scaffolded to this Aaeg L5 genome.

Genome Annotation. We first identified and masked repetitive elements in our reference genome assembly using RepeatModeler v2.0.1 with a custom repeat library (132) and RepeatMasker 4.1.6. (133). We then annotated the genome for protein-coding genes using *BRAKER2*–a fully automated pipeline that uses the tools *GENEMARK-ES/ET* (134) and *AUGUSTUS* (135) for gene structure prediction (136). Specifically, we conducted *ab initio* gene prediction in BRAKER2 v2.1.6, using the genome file only (i.e., without additional evidence from RNA-Seq or protein data, as these are unavailable) and a minimum contig length of 10,000.

Read Trimming and Variant Calling. Raw reads were first quality filtered and trimmed using *Trimmomatic* v0.39 (137) with the following parameters: ILLUMINACLIP:TruSeq3-PE.fa:2:30:10 LEADING:3 TRAILING:3 MINLEN:35 SLIDINGWINDOW:4:15. We then aligned these reads to the scaffolded reference genome using *BWA-MEM* v0.7.12, with default parameters (138). We marked and removed duplicate reads using *picard* v2.0.1. We then identified SNPs in our samples using *bcftools* v1.18 (139) and filtered variants using *vcftools* v0.1.16 (140) with the following parameters: minor allele frequency of 0.05, minimum depth of 10×, minimum average quality of 40, and a maximum variant missing of 0.995. We then filtered out any SNPs with multiple alleles using *bcftools*, keeping only biallelic polymorphisms. This retained 3,564,483 SNPs. As large linkage blocks have been found in related *Aedes* species (141), we filtered for linkage disequilibrium (LD) in this SNP set using an LD-based SNP pruning algorithm in *plink* v1.9 (142). Specifically, we used a sliding window of 50 SNPs, a window shift increment of five SNPs, and variance inflation factor of 1.5, which

corresponds to an R^2 of 0.3 for the focal SNP regressed against all other SNPs in the window (143, 144). This yielded 583,889 independent SNPs that were retained for downstream analysis.

Population Diversity Metrics. To estimate the genetic diversity of our starting population, we calculated the individual-level heterozygosity and population-level nucleotide diversity (π) in 10 kb windows using *vcftools* v0.1.16 (140). We estimated these metrics using only the control individuals that survived to adulthood, as representative of the population prior to heat selection.

Identifying Genetic Variants Associated with Heat Tolerance. To investigate the genetic basis of heat tolerance, we used a combination of PCA (*SI Appendix*, Figs. S10 and S11), statistical tests of genomic differentiation (F_{st}), and GWA approaches. We first visualized overall genomic variation through PCA on the allele frequency matrix (after centering and scaling) using the *prcomp* function in R. We used these PCA visualizations to briefly explore whether there was a dominant signal of treatment or sex, as well as experimental round, as a quality control measure (*SI Appendix*, Figs. S10 and S11). We then detected candidate SNPs underlying heat tolerance using the following approaches: 1) genomic differentiation (F_{st}) between control and heat-selected individuals, 2) a case–control GWA analysis between control and heat-selected individuals, and 3) GWA using knockdown time as the phenotype. Approaches one and two are aimed at identifying genetic variants associated with tolerance to prolonged heat exposure during development. We adopted two independent but complementary approaches to compare SNPs identified under the varying assumptions of each method and to ultimately refine the candidate SNP list (i.e., SNPs identified by both approaches are less likely to be false positives). Approach three is designed to detect variants associated with acute heat tolerance at the adult life stage using a standard GWA approach (i.e., regression of continuous trait value on genotype status).

Approach one (F_{st}-based approach) was implemented using R package *OutFLANK* v0.2, which calculates F_{st} at each SNP using the Weir and Cockerham method (145) and then identifies SNPs that deviate from an inferred neutral F_{st} distribution (146). We considered SNPs below a q-value threshold of 0.05 and with $F_{st} > 0.05$ as candidate SNPs putatively underlying heat tolerance. Our second approach to identify SNPs associated with prolonged, larval thermal tolerance was a modified GWA, whereby the "phenotype" used in the regression was the treatment of the sequenced individual. We implemented a logistic regression and included sex as a covariate to control for sex-specific variation in mosquito heat tolerance (Andersen et al. (147)), using *plink* v1.9 (142). Finally, we conducted a standard GWA for adult, acute thermal tolerance using knockdown time as the phenotype, and sex, treatment, and wing length as covariates to account for effects of larval rearing temperatures and body size on acute adult heat tolerance (74) (also conducted using *plink* v1.9). To correct for residual LD in both GWA-based approaches, we performed an LD-based "clumping" procedure, wherein SNP-based results from the association analyses are grouped based on estimates of LD between SNPs. We implemented this procedure in *plink* using default parameters (i.e., 0.0001 significance threshold for the focal SNP, 0.01 significance threshold for clumped SNPs, 0.50 R2 threshold for clumping, and a 250 kb window for clumping). We defined candidate SNPs as those with $P < 0.01$ after Benjamini–Hochberg FDR correction.

To identify the genes associated with these candidate SNPs, we assigned SNPs to genes based on their position and the BRAKER gene annotation. For SNPs that did not fall within a BRAKER-annotated gene, we assigned it to the closest gene if this was within 50 kb, otherwise we removed it from downstream analysis on candidate gene overlap and function.

Using the candidate gene list from each approach, we then investigated the genomic basis of prolonged versus acute heat exposure. Specifically, we compared the genes identified through F_{st} or GWA on control and heat-selected individuals (i.e., representing prolonged heat exposure), and through GWA on knockdown time (i.e., representing acute heat exposure). Next, we sought to determine whether the number of shared genes identified by these approaches was more or less than that expected by chance, to identify candidate genes identified by multiple independent approaches, and determine whether the pathways related to heat tolerance between life-stages (and at long-term versus acute scales) were similar. To do so, we developed a null distribution of gene overlap by drawing random samples from the available gene set wherein, for each focal gene, we selected a random gene that was a) on the same chromosome and b) within one SD of gene length. We did this for the focal genes identified through each approach, then determined the number of overlapping genes in each of 500 iterations to generate a null distribution of gene overlap. If the true overlap between genes identified in each approach was greater than the expectation based on this null distribution, we inferred that the approaches were identifying shared pathways.

Last, to identify the putative biological function of focal genes identified herein, we mapped the gene sequences to annotated transcriptomes of related *Aedes* species (i.e., *A. albopictus,* NCBI accession: GCF_006496715.1; *A. aegypti,* NCBI accession: GCF_002204515.2) using BLASTN. In the case of multiple hits for a given sequence, we used the result with the lowest E-value and highest Max score.

Investigating Structural Variation. We used four short-read structural variant callers, *Manta* v1.6.0, *Delly2* v1.2.6, *Lumpy* (via *smoove* v0.2.8), and *GRIDSS2* v2.13.2, to identify inversions in each of our samples (148–151). *GRIDSS2* was run with the flag --skipsoftcliprealignment, while the other three callers were run with default settings. For each sample, the sets of variants from each of the four callers were merged together with *Jasmine* v1.1.5, requiring support from at least three callers to keep a variant in the final set for that sample (using the min_support=3 argument) (152). Finally, variant sets from all samples were merged into a single, population-level VCF with *Jasmine*. In both instances, *Jasmine* was run with the arguments spec_reads=8, spec_len=35, --dup-to-ins --mark-specific, and --normalize-type. For each consensus inversion, individuals were labeled as "0" (homozygous no inversion) or "1" (homozygous for inversion or heterozygous), as short-read variant callers such as those used here may not accurately call heterozygosity (153). To minimize spurious detection (e.g., due to misalignment of transposable elements or repetitive sequences), the full set of variants across samples was filtered to only include inversions of size 1 to 200 Mb and frequency >5% in the population (n = 89) with *bcftools* v1.17 and custom bash scripts.

To identify inversions that may be associated with heat tolerance, we compared the frequency of each inversion between either the control and heat-selected individuals or between individuals from the top 25% and bottom 25% of knockdown times (controlling for treatment and sex) using a chi-squared test. We then compared the observed chi-squared test statistic to that obtained after randomly shuffling the group labels (n = 500 permutations). We considered inversions as significantly differentiated between groups if their observed chi-squared test statistic was above the 95% CI for the test statistic from the permutations, after Bonferroni adjustment for multiple testing. Next, to compare the genomic position of inversions and candidate SNPs, we investigated whether inversions occurred in specific chromosomal regions in which we observed an elevated number of SNPs associated with larval heat tolerance (Fig. 2*A* and *SI Appendix*, Fig. S3). These regions of interest were explicitly defined based on SNP signals within sliding windows following methods of ref. 154 (*SI Appendix, Supplemental Methods*).

Due to limitations in short-read variants callers, we used a localized PCA approach to test the hypothesis that inversions are present within the regions with elevated SNP signal. Specifically, if inversions were indeed present in these regions, we would expect to see a trimodal distribution of points in principal components space, representing the standard, inverted, and heterozygotes haplotypes (48). Such a pattern is expected as distinct inversion haplotypes should share combinations of SNPs that generate a clustering of individuals in genotypic space via dimensionality reduction of SNP data, such as PCA. While this signal may be masked by variation at loci outside of inversions when conducting PCA genome-wide, a localized approach may be sufficiently resolved to detect the clustering of inversion haplotypes (48).

Estimating Allele Frequency Shifts. For candidate loci underlying differences between control and heat-selected individuals, we investigated shifts in allele frequencies between these groups, relative to a set of matched controls. For each focal SNP, we generated a random set of 10 matched control SNPs with the following criteria: presence on the same chromosome, ±2.5% baseline allele frequency (i.e., allele frequency in the control individuals), and at least 100 kb away from the focal SNP (to account for LD). We then compared differences in the distribution of allele frequency shifts in the focal SNPs relative to their matched controls using a Kolmogorov–Smirnov test, and compared shifts in allele frequency based on starting median allele frequency (*SI Appendix*, Fig. S4). We repeated this process

to investigate allele frequency differences between individuals with high (upper 50% of phenotypic distribution) or low (bottom 50%) knockdown times relative to their treatment and sex. Herein, for each focal SNP identified from the GWA on knockdown time, we generated a set of 10 matched controls based on presence on the same chromosome and at least 100 kbps separation from the focal SNP.

Estimating Adaptive Potential. To investigate whether the standing variation in thermal tolerance observed here may enable adaptation to climate warming, we used an evolutionary rescue model framework (17, 64, 65). These models compare the maximum potential rate of evolutionary change for a population to the projected rate of environmental change. If evolutionary rates exceed that of environmental change, populations may persist through evolutionary adaptation (97, 155–158). Evolutionary rescue models have provided useful estimates of climate adaptive potential across a variety of taxa (159–162). However, there are few examples of their validation in natural settings, thus we pose this analysis as a means of estimating adaptive potential under idealized and simplified conditions that warrant further investigation under more ecologically realistic settings, rather than an attempt to estimate a precise rate of warming to which mosquito populations may adapt. Here, we specifically consider the rate of evolutionary change in the thermal tolerance of larval survival and compare it to rates of change in mean daily temperatures in the larval activity period (January – April) as projected under a moderate warming scenario for the southern portion of the *A. sierrensis* distribution (discussed further below). We focus on larval thermal tolerance as our recent investigation of thermal tolerance across the life stages of this species indicates that larval survival may be the bottleneck to adaptation (19). We use the analytic, quantitative-genetic formulation of the evolutionary rescue model below, based on refs. 64 and 65 (see *SI Appendix, Supplemental Methods* for derivation).

$$\eta_c = \sqrt{\frac{2\, r_{max}\, \gamma}{T}} \times h^2 \sigma_p^2. \quad [1]$$

Here, η_c is the maximum rate of environmental change under which the population could persist (which is equivalent to the maximum rate of adaptive evolution), r_{max} is the maximum rate of population growth under optimal conditions, γ is the strength of selection, T is the generation time, h^2 is the heritability of the trait, and σ_p^2 is the phenotypic variance. We note that this formulation does not incorporate phenotypic plasticity, which could modify the strength of selection and rate of change in the trait under warming (64).

We parameterized the model using estimates from our experimental and genomic results, and prior estimates of maximum mosquito population growth rate and *A. sierrensis* generation time (*SI Appendix*, Table S8). Namely, prior studies have estimated r_{max} for *A. aegypti*, *A. gambiae*, and *Culex pipiens* as 0.24 to 0.335, 0.187, 0.379, respectively, based on laboratory experiments that varied larval competition and/or temperature (17, 163, 164). As r_{max} for mosquito populations in natural settings remains largely unknown, we estimate adaptive potential over a range of r_{max} from 0.15 to 0.35, based on these prior estimates. We estimated the strength of selection, γ, as the difference in larval survival between treatments [i.e., $\gamma = 1 -$ (survival in heat-selected group/survival in control group)] (165) across all experimental rounds collectively ($\gamma = 0.578$), as well as each individual experimental round ($\gamma = 0.463, 0.606, 0.590$). An important limitation in our parameterization of γ is that it was not estimated under the same temperature conditions as expected under warming. That is, we estimated selection strength by comparing larval survival at 22 and 30 °C, which approximately capture the maximum temperature this population may experience in the spring (the larval activity period) and the upper thermal limits for larval survival as measured under constant temperatures (19), indicating the selective regime we imposed is likely to be biologically realistic. However, this temperature differential may be larger than that experienced by natural populations in coming decades, causing us to overestimate selection strength (though this estimate may also be an underestimate during extreme heat events when temperatures far exceed expected mean shifts). However, in the absence of theoretical or experimental approaches to estimate γ under environmental conditions that are changing continuously and nonlinearly with respect to time, we use the estimate of γ made here and interpret our results cautiously. To estimate heritability and phenotypic variance, we used *GCTA*–a tool developed to estimate these parameters for complex traits based on genome-wide SNPs (166). First, the pairwise genetic relatedness between all individuals is estimated based on all SNPs. As the *GCTA* method relies heavily on LD between SNPs, and can overestimate heritability under certain LD scenarios, we performed this step using the SNP list both before and after LD-pruning (*Materials and Methods, Read Trimming and Variant Calling*). The resulting genetic relationship matrix is then used to estimate the variance in the larval heat tolerance phenotype explained by the SNPs using restricted maximum likelihood. Herein, all SNPs are used, rather than solely those identified as focal SNPs from F_{st} or GWA approaches, to avoid overestimating effect sizes (i.e., the "Winner's Curse" issue in genetic association studies) (167). We included sex as a covariate in this estimation to control for any sex-specific differences in survival.

We compared the estimated maximum rate of evolutionary change based on our parameter estimates (*SI Appendix*, Table S8), to rates of change in mean daily temperature in the spring (here, January – April)–the period when larvae are developing. Specifically, we estimated the rate of warming in spring temperatures between 2020 and 2050 under a moderate warming scenario (RCP 4.5) across the southern portion of the *A. sierrensis* distribution, based on California vector surveillance data for the past decade (*SI Appendix*, Fig. S13). Surveillance data were obtained from the CalSurv Gateway through data request 000045 approved on October 19, 2020, by the California Vectorborne Diseases Surveillance System. We consider this to be the most ecologically relevant metric of warming, but to ensure our results were not specific to this precise metric of warming, we also considered alternative metrics (*SI Appendix*, Table S9).

Data, Materials, and Software Availability. All R scripts, bioinformatic scripts, and intermediate and final analysis files are available in an external data repository hosted on GitHub: https://github.com/lcouper/MosquitoThermalSelection (168).

ACKNOWLEDGMENTS. We gratefully acknowledge Bret Barner, Kristen Holt, and Angie Nakano from California vector control agencies for assisting with larval sampling and optimizing mosquito-rearing protocols. We thank Kelsey Lyberger and Johannah Farner for assisting with mosquito rearing and Dmitri Petrov, Molly Schumer, and members of the Moi lab for providing insights that helped shape the analytical approaches herein. This work was supported by the Philippe Cohen Graduate Fellowship, the Pacific Southwest Center of Excellence in Vector-Borne Diseases Training Grant, and the NSF graduate research fellowship awarded to T.O.D. E.A.M. was supported by NSF grant DEB-2011147 with Fogarty International Center, NIH grants R35GM133439, R01AI168097, and R01AI102918, and seed grants from the Stanford Doerr School of Sustainability, Woods Institute for the Environment, King Center on Global Development, and Center for Innovation in Global Health.

Author affiliations: [a]Department of Biology, Stanford University, Stanford, CA 94305; [b]Division of Environmental Health Sciences, University of California, Berkeley, CA 94704; [c]Department of Integrative Biology, University of California, Berkeley, CA 94704; [d]HHMI, Chevy Chase, MD 20815; and [e]Department of Plant & Microbial Biology, University of California, Berkeley, CA 94704

1. A. M. Kilpatrick, S. E. Randolph, Drivers, dynamics, and control of emerging vector-borne zoonotic diseases. *Lancet* **380**, 1946–1955 (2012).
2. J. N. Mills, K. L. Gage, A. S. Khan, Potential influence of climate change on vector-borne and zoonotic diseases: A review and proposed research plan. *Environ. Health Perspect.* **118**, 1507–1514 (2010).
3. M. A. Kulkarni, C. Duguay, K. Ost, Charting the evidence for climate change impacts on the global spread of malaria and dengue and adaptive responses: A scoping review of reviews. *Glob. Health* **18**, 1 (2022).
4. S. J. Ryan, Mapping thermal physiology of vector-borne diseases in a changing climate: Shifts in geographic and demographic risk of suitability. *Curr. Environ. Health Rep.* **7**, 415–423 (2020).
5. S. J. Ryan, C. J. Carlson, E. A. Mordecai, L. R. Johnson, Global expansion and redistribution of Aedes-borne virus transmission risk with climate change. *PLoS Negl. Trop. Dis.* **13**, e0007213 (2019).
6. World Health Organization, "A global brief on vector-borne diseases" (Geneva, Switzerland, 2014).
7. C. J. Carlson *et al.*, Rapid range shifts in African Anopheles mosquitoes over the last century. *Biol. Lett.* **19** (2023).
8. M. A. Kulkarni *et al.*, 10 years of environmental change on the slopes of Mount Kilimanjaro and its associated shift in malaria vector distributions. *Front. Public Health* **4**, 1–10 (2016).
9. L. L. Pinault, F. F. Hunter, New highland distribution records of multiple Anopheles species in the Ecuadorian Andes. *Malar. J.* **10**, 236 (2011).

10. M. C. Pedrosa *et al.*, Invasion of tropical montane cities by Aedes aegypti and Aedes albopictus (Diptera: Culicidae) depends on continuous warm winters and suitable urban biotopes. *J. Med. Entomol.* **58**, 333–342 (2021).
11. M. Equihua *et al.*, Establishment of Aedes aegypti (L.) in mountainous regions in Mexico: Increasing number of population at risk of mosquito-borne disease and future climate conditions. *Acta Trop.* **166**, 316–327 (2017).
12. M. U. G. Kraemer *et al.*, Past and future spread of the arbovirus vectors Aedes aegypti and Aedes albopictus. *Nat. Microbiol.* **4**, 854–863 (2019).
13. M. Mogi, N. Tuno, Impact of climate change on the distribution of Aedes albopictus (Diptera: Culicidae) in Northern Japan: Retrospective analyses. *J. Med. Entomol.* **51**, 572–579 (2014).
14. J. Kasper, B. Tomotani, A. Hovius, M. McIntyre, M. Musicante, Changing distributions of the cosmopolitan mosquito species Culex quinquefasciatus Say and endemic Cx. pervigilans Bergroth (Diptera: Culicidae) in New Zealand. *N. Z. J. Zool.* **50**, 406–424 (2022).
15. D. Roth *et al.*, West Nile virus range expansion into British Columbia. *Emerg. Infect. Dis.* **16**, 1251–1258 (2010).
16. R. F. Andriamifidy, N. B. Tjaden, C. Beierkuhnlein, S. M. Thomas, Do we know how mosquito disease vectors will respond to climate change? *Emerg. Top. Life Sci.* **3**, 115–132 (2019).
17. L. I. Couper *et al.*, How will mosquitoes adapt to climate warming? *Elife* **10**, e69630 (2021).
18. L. H. V. Franklinos, K. E. Jones, D. W. Redding, I. Abubakar, The effect of global change on mosquito-borne disease. *Lancet Infect. Dis.* **19**, e302–e312 (2019).
19. L. I. Couper, J. E. Farner, K. P. Lyberger, A. S. Lee, E. A. Mordecai, Mosquito thermal tolerance is remarkably constrained across a large climatic range. *Proc. R. Soc. B* **291** (2024).
20. V. M. Chu *et al.*, Regional variation in life history traits and plastic responses to temperature of the major malaria vector Nyssorhynchus darlingi in Brazil. *Sci. Rep.* **9**, 5356 (2019).
21. B. L. Dodson, L. D. Kramer, J. L. Rasgon, Effects of larval rearing temperature on immature development and West Nile virus vector competence of Culex tarsalis. *Parasites Vectors* **5**, 199 (2012).
22. W. Reisen, Effect of temperature on Culex tarsalis (Diptera: Culicidae) from the Coachella and San Joaquin Valleys of California. *J. Med. Entomol.* **32**, 636–645 (1995).
23. J. E. Ruybal, L. D. Kramer, A. M. Kilpatrick, Geographic variation in the response of Culex pipiens life history traits to temperature. *Parasites Vectors* **9**, 116 (2016).
24. A. S. Vorhees, E. M. Gray, T. J. Bradley, Thermal resistance and performance correlate with climate in populations of a widespread mosquito. *Physiol. Biochem. Zool.* **86**, 73–81 (2013).
25. P. A. Zani *et al.*, Geographic variation in tolerance of transient thermal stress in the mosquito Wyeomyia smithii. *Ecology* **86**, 1206–1211 (2005).
26. N. L. Dennington *et al.*, Phenotypic adaptation to temperature in the mosquito vector, Aedes aegypti. *Glob. Change Biol.* **30**, e17041 (2024).
27. F. Ware-Gilmore, M. Novelo, C. M. Sgrò, M. D. Hall, E. A. McGraw, Assessing the role of family level variation and heat shock gene expression in the thermal stress response of the mosquito Aedes aegypti. *Philos. Trans. R. Soc. B* **378**, 20220011 (2023).
28. D. E. Terasaki Hart, I. J. Wang, Genomic architecture controls multivariate adaptation to climate change. *Glob. Change Biol.* **30**, e17179 (2024).
29. M. Yamamichi, How does genetic architecture affect eco-evolutionary dynamics? A theoretical perspective *Philos. Trans. R. Soc. B* **377**, 20200504 (2022).
30. L.-J. Ma *et al.*, Rapid and repeated climate adaptation involving chromosome inversions following invasion of an insect. *Mol. Biol. Evol.* **41**, msae044 (2024).
31. N. Barghi, J. Hermisson, C. Schlötterer, Polygenic adaptation: A unifying framework to understand positive selection. *Nat. Rev. Genet.* **21**, 769–781 (2020).
32. E. R. Hager *et al.*, A chromosomal inversion contributes to divergence in multiple traits between deer mouse ecotypes. *Science* **377**, 399–405 (2022).
33. N. H. Rose, R. A. Bay, M. K. Morikawa, S. R. Palumbi, Polygenic evolution drives species divergence and climate adaptation in corals. *Evolution* **72**, 82–94 (2018).
34. K. Csilléry, A. Rodríguez-Verdugo, C. Rellstab, F. Guillaume, Detecting the genomic signal of polygenic adaptation and the role of epistasis in evolution. *Mol. Ecol.* **27**, 606–612 (2018).
35. T. M. Healy, R. S. Brennan, A. Whitehead, P. M. Schulte, Tolerance traits related to climate change resilience are independent and polygenic. *Glob. Change Biol.* **24**, 5348–5360 (2018).
36. A. A. Hoffmann, C. M. Sgrò, A. R. Weeks, Chromosomal inversion polymorphisms and adaptation. *Trends Ecol. Evol.* **19**, 482–488 (2004).
37. M. Wellenreuther, L. Bernatchez, Eco-evolutionary genomics of chromosomal inversions. *Trends Ecol. Evol.* **33**, 427–440 (2018).
38. C. Fouet, E. Gray, N. J. Besansky, C. Costantini, Adaptation to aridity in the malaria mosquito Anopheles gambiae: Chromosomal inversion polymorphism and body size influence resistance to desiccation. *PLoS One* **7**, e34841 (2012).
39. S. T. Small *et al.*, Standing genetic variation and chromosome differences drove rapid ecotype formation in a major malaria mosquito. *Proc. Natl. Acad. Sci. U.S.A.* **120**, e2219835120 (2023).
40. D. Ayala, A. Ullastres, J. González, Adaptation through chromosomal inversions in Anopheles. *Front. Genet.* **5**, 1–10 (2014).
41. M. Coluzzi, A. Sabatini, V. Petrarca, M. A. Di Deco, Chromosomal differentiation and adaptation to human environments in the Anopheles gambiae complex. *Trans. R. Soc. Trop. Med. Hyg.* **73**, 483–497 (1979).
42. M. Coluzzi, A. Sabatini, A. della Torre, M. A. Di Deco, V. Petrarca, A polytene chromosome analysis of the Anopheles gambiae species complex. *Science* **298**, 1415–1418 (2002).
43. B. J. White *et al.*, Localization of candidate regions maintaining a common polymorphic inversion (2La) in Anopheles gambiae. *PLoS Genet.* **3**, e217 (2007).
44. E. M. Gray, K. A. Rocca, C. Costantini, N. J. Besansky, Inversion 2La is associated with enhanced desiccation resistance in Anopheles gambiae. *Malar. J.* **8**, 215 (2009).
45. K. L. Bennett, W. O. McMillan, J. R. Loaiza, The genomic signal of local environmental adaptation in Aedes aegypti mosquitoes. *Evol. Appl.* **14**, 1301–1313 (2021).
46. S. A. Bernhardt, C. Blair, M. Sylla, C. Bosio, W. C. Black IV, Evidence of multiple chromosomal inversions in Aedes aegypti formosus from Senegal. *Insect Mol. Biol.* **18**, 557–569 (2009).
47. S. N. Redmond *et al.*, Linked-read sequencing identifies abundant microinversions and introgression in the arboviral vector Aedes aegypti. *BMC Biol.* **18**, 26 (2020).
48. J. Liang *et al.*, Discovery and characterization of chromosomal inversions in the arboviral vector mosquito Aedes aegypti. bioXriv [Preprint] (2024). https://www.biorxiv.org/content/10.1101/2024.02.16.580682v. Accessed 17 November 2024.
49. R. F. Darsie, R. A. Ward, Identification and geographical distribution of the mosquitoes of North America, north of Mexico. *Mosq. Syst.* **327**, 1–313 (1981).
50. F. Ware-Gilmore *et al.*, Microbes increase thermal sensitivity in the mosquito Aedes aegypti, with the potential to change disease distributions. *PLoS Negl. Trop. Dis.* **15**, e0009548 (2021).
51. B. F. Oliveira, W. I. G. Yogo, D. A. Hahn, J. Yongxing, B. R. Scheffers, Community-wide seasonal shifts in thermal tolerances of mosquitoes. *Ecology* **102**, e03368 (2021).
52. K. Lyberger, J. E. Farner, L. Couper, E. A. Mordecai, Plasticity in mosquito size and thermal tolerance across a latitudinal climate gradient. *J. Anim. Ecol.* (2024).
53. A. A. Hoffmann, L. H. Rieseberg, Revisiting the impact of inversions in evolution: From population genetic markers to drivers of adaptive shifts and speciation? *Annu. Rev. Ecol. Evol. Syst.* **39**, 21–42 (2008).
54. C. Cheng *et al.*, Ecological genomics of Anopheles gambiae along a latitudinal cline: A population-resequencing approach. *Genetics* **190**, 1417–1432 (2012).
55. C. Cheng, J. C. Tan, M. W. Hahn, N. J. Besansky, Systems genetic analysis of inversion polymorphisms in the malaria mosquito Anopheles gambiae. *Proc. Natl. Acad. Sci. U.S.A.* **115**, E7005–E7014 (2018).
56. L. Pratx, P. Wendering, C. Kappel, Z. Nikoloski, I. Bäurle, Histone retention preserves epigenetic marks during heat stress-induced transcriptional memory in plants. *EMBO J.* **42**, e113595 (2023).
57. A. Pajoro, E. Severing, G. C. Angenent, R. G. H. Immink, Histone H3 lysine 36 methylation affects temperature-induced alternative splicing and flowering in plants. *Genome Biol.* **18**, 102 (2017).
58. H. Son *et al.*, Functional characterization of an Arabidopsis profilin protein as a molecular chaperone under heat shock stress. *Molecules* **27**, 5771 (2022).
59. T. Fan, R. Wang, Y. Xiang, L. An, S. Cao, Heat stress induces actin cytoskeletal reorganization and transcript profiles of vegetative profilins and actin depolymerizing factors (ADFs) in Arabidopsis. *Acta Physiol. Plant.* **38**, 37 (2016).
60. B. A. Pandian, R. Sathishraj, M. Djanaguiraman, P. V. V. Prasad, M. Jugulam, Role of cytochrome P450 enzymes in plant stress response. *Antioxidants* **9**, 454 (2020).
61. N. N. Rosic, M. Pernice, S. Dunn, S. Dove, O. Hoegh-Guldberg, Differential regulation by heat stress of novel cytochrome P450 genes from the dinoflagellate symbionts of reef-building corals. *Appl. Environ. Microbiol.* **76**, 2823–2829 (2010).
62. X. Shen, W. Liu, F. Wan, Z. Lv, J. Guo, The role of cytochrome P450 4C1 and carbonic anhydrase 3 in response to temperature stress in Bemisia tabaci. *Insects* **12**, 1071 (2021).
63. A. Egizi, N. H. Fefferman, D. M. Fonseca, Evidence that implicit assumptions of 'no evolution' of disease vectors in changing environments can be violated on a rapid timescale. *Philos. Trans. R. Soc. B* **370**, 20140136 (2015).
64. L.-M. Chevin, R. Lande, G. M. Mace, Adaptation, plasticity, and extinction in a changing environment: Towards a predictive theory. *PLoS Biol.* **8** (2010).
65. M. Lynch, R. Lande, Evolution and extinction in response to environmental change. *Biotic Interact. Glob. Change* **49**, 234–250 (1993).
66. K. Bowler, Acclimation, heat shock and hardening. *J. Therm. Biol.* **30**, 125–130 (2005).
67. A. R. Gunderson, M. E. Dillon, J. H. Stillman, Estimating the benefits of plasticity in ectotherm heat tolerance under natural thermal variability. *Funct. Ecol.* **31**, 1529–1537 (2017).
68. A. R. Gunderson, J. H. Stillman, Plasticity in thermal tolerance has limited potential to buffer ectotherms from global warming. *Proc. R. Soc. B* **282**, 20150401 (2015).
69. T. M. Healy, A. K. Bock, R. S. Burton, Variation in developmental temperature alters adulthood plasticity of thermal tolerance in Tigriopus californicus. *J. Exp. Biol.* **222**, jeb213405 (2019).
70. S. A. Morley, L. S. Peck, J. Sunday, S. Heiser, A. E. Bates, Physiological acclimation and persistence of ectothermic species under extreme heat events. *Glob. Ecol. Biogeogr.* **28**, 1018–1037 (2019).
71. N. E. Moyen, R. L. Crane, G. N. Somero, M. W. Denny, A single heat-stress bout induces rapid and prolonged heat acclimation in the California mussel, Mytilus californianus. *Proc. Biol. Sci.* **287**, 20202561 (2020), 10.1098/rspb.2020.2561.
72. N. E. Moyen, G. N. Somero, M. W. Denny, Effects of heat acclimation on cardiac function in the intertidal mussel Mytilus californianus: Can laboratory-based indices predict survival in the field? *J. Exp. Biol.* **225**, jeb243050 (2022).
73. P. Pottier *et al.*, Developmental plasticity in thermal tolerance: Ontogenetic variation, persistence, and future directions. *Ecol. Lett.* **25**, 2245–2268 (2022).
74. H. I. Sasmita, W.-C. Tu, L.-J. Bong, K.-B. Neoh, Effects of larval diets and temperature regimes on life history traits, energy reserves and temperature tolerance of male Aedes aegypti (Diptera: Culicidae): Optimizing rearing techniques for the sterile insect programmes. *Parasites Vectors* **12**, 578 (2019).
75. A. G. Gibbs, A. K. Louie, J. A. Ayala, Effects of temperature on cuticular lipids and water balance in a desert Drosophila: Is thermal acclimation beneficial. *J. Exp. Biol.* **201**, 71–80 (1998).
76. L. S. Peck, M. S. Clark, S. A. Morley, A. Massey, H. Rossetti, Animal temperature limits and ecological relevance: Effects of size, activity and rates of change. *Funct. Ecol.* **23**, 248–256 (2009).
77. I. Peralta-Maraver, E. L. Rezende, Heat tolerance in ectotherms scales predictably with body size. *Nat. Clim. Chang.* **11**, 58–73 (2021).
78. E. L. Rezende, L. E. Castañeda, M. Santos, Tolerance landscapes in thermal ecology. *Funct. Ecol.* **28**, 799–809 (2014).
79. A. A. Hoffmann, S. L. Chown, S. Clusella-Trullas, Upper thermal limits in terrestrial ectotherms: How constrained are they? *Funct. Ecol.* **27**, 934–949 (2013).
80. T. J. K. Strang, A review of published temperatures for the control of pest insects in museums. *Collect. Forum* **8**, 41–67 (1992).
81. J. M. Sunday, A. E. Bates, N. K. Dulvy, Global analysis of thermal tolerance and latitude in ectotherms. *Proc. R. Soc. B* **278**, 1823–1830 (2010).
82. M. M. Riehle *et al.*, The Anopheles gambiae 2La chromosome inversion is associated with susceptibility to Plasmodium falciparum in Africa. *Elife* **6**, e25813 (2017).
83. R. Faria, K. Johannesson, R. K. Butlin, A. M. Westram, Evolving inversions. *Trends Ecol. Evol.* **34**, 239–248 (2019).
84. M. Kirkpatrick, N. Barton, Chromosome inversions, local adaptation and speciation. *Genetics* **173**, 419–434 (2006).
85. A. della Torre, L. Merzagora, J. R. Powell, M. Coluzzi, Selective introgression of paracentric inversions between two sibling species of the Anopheles gambiae complex. *Genetics* **146**, 239–244 (1997).
86. N. J. Besansky *et al.*, Semipermeable species boundaries between Anopheles gambiae and Anopheles arabiensis: Evidence from multilocus DNA sequence variation. *Proc. Natl. Acad. Sci. U.S.A.* **100**, 10818–10823 (2003).
87. F. J. Ayala, M. Coluzzi, Chromosome speciation: Humans, Drosophila, and mosquitoes. *Proc. Natl. Acad. Sci. U.S.A.* **102**, 6535–6542 (2005).
88. M. L. Sottile, S. B. Nadin, Heat shock proteins and DNA repair mechanisms: An updated overview. *Cell Stress Chaperones* **23**, 303–315 (2018).

89. M. B. S. Mota, M. A. Carvalho, A. N. A. Monteiro, R. D. Mesquita, DNA damage response and repair in perspective: Aedes aegypti, Drosophila melanogaster and Homo sapiens. *Parasites Vectors* **12**, 533 (2019).
90. C. Vinauger *et al.*, Visual-olfactory integration in the human disease vector mosquito Aedes aegypti. *Curr. Biol.* **29**, 2509–2516.e5 (2019).
91. L. M. Gomulski *et al.*, Transcriptional variation of sensory-related genes in natural populations of Aedes albopictus. *BMC Genomics* **21**, 547 (2020).
92. R. Parkash, D. D. Aggarwal, P. Ranga, D. Singh, Divergent strategies for adaptation to desiccation stress in two Drosophila species of immigrans group. *J. Comp. Physiol. B* **182**, 751–769 (2012).
93. S. Ramniwas, B. Kajla, Divergent strategy for adaptation to drought stress in two sibling species of montium species subgroup: Drosophila kikkawai and Drosophila leontia. *J. Insect Physiol.* **58**, 1525–1533 (2012).
94. M. Santos, L. E. Castañeda, E. L. Rezende, Making sense of heat tolerance estimates in ectotherms: Lessons from Drosophila. *Funct. Ecol.* **25**, 1169–1180 (2011).
95. J. S. Terblanche, J. A. Deere, S. Clusella-Trullas, C. Janion, S. L. Chown, Critical thermal limits depend on methodological context. *Proc. R. Soc. B* **274**, 2935–2943 (2007).
96. H. Padmanabha, C. C. Lord, L. P. Lounibos, Temperature induces trade-offs between development and starvation resistance in Aedes aegypti (L.) larvae. *Med. Vet. Entomol.* **25**, 445–453 (2011).
97. A. A. Hoffmann, C. M. Sgrò, Climate change and evolutionary adaptation. *Nature* **470**, 479–485 (2011).
98. D. D. Chadee, R. Martinez, Aedes aegypti (L.) in Latin American and Caribbean region: With growing evidence for vector adaptation to climate change? *Acta Trop.* **156**, 137–143 (2016).
99. J. H. Stillman, Acclimation capacity underlies susceptibility to climate change. *Science* **301**, 65–65 (2003).
100. B. Van Heerwaarden, V. Kellermann, Does plasticity trade off with basal heat tolerance? *Trends Ecol. Evol.* **35**, 874–885 (2020).
101. J. M. Barley *et al.*, Limited plasticity in thermally tolerant ectotherm populations: Evidence for a trade-off. *Proc. R. Soc. B* **288**, 20210765 (2021).
102. J. G. Kingsolver, L. B. Buckley, Evolution of plasticity and adaptive responses to climate change along climate gradients. *Proc. R. Soc. B* **284**, 20170386 (2017).
103. S. Salinas, S. E. Irvine, C. L. Schertzing, S. Q. Golden, S. B. Munch, Trait variation in extreme thermal environments under constant and fluctuating temperatures. *Philos. Trans. R. Soc. B* **374**, 20180177 (2019).
104. A. Husby, M. E. Visser, L. E. B. Kruuk, Speeding up microevolution: The effects of increasing temperature on selection and genetic variance in a wild bird population. *PLoS Biol.* **9**, e1000585 (2011).
105. J. Polechová, N. H. Barton, Limits to adaptation along environmental gradients. *Proc. Natl. Acad. Sci. U.S.A.* **112**, 6401–6406 (2015).
106. J. R. Bridle, J. Polechová, M. Kawata, R. K. Butlin, Why is adaptation prevented at ecological margins? New insights from individual-based simulations *Ecol. Lett.* **13**, 485–494 (2010).
107. F. Simard *et al.*, Ecological niche partitioning between Anopheles gambiae molecular forms in Cameroon: The ecological side of speciation. *BMC Ecol.* **9**, 17 (2009).
108. E. A. Mordecai, S. J. Ryan, J. M. Caldwell, M. M. Shah, A. D. LaBeaud, Climate change could shift disease burden from malaria to arboviruses in Africa. *Lancet Planet. Health* **4**, e416–e423 (2020).
109. R. G. Jordan, W. E. Bradshaw, Geographic variation in the photoperiodic response of the Western tree-hole mosquito, Aedes sierrensis. *Ann. Entomol. Soc. Am.* **71**, 487–490 (1978).
110. N. US Department of Commerce, National Weather Service, National Weather Service: Fairfield/Travis Air Force Base (KSUU). (2024). https://forecast.weather.gov/MapClick.php?lat=38.2669&lon=-121.94. Accessed 28 August 2024.
111. J. J. Berg *et al.*, Reduced signal for polygenic adaptation of height in UK Biobank. *Elife* **8**, e39725 (2019).
112. D. C. Hardie, J. A. Hutchings, Evolutionary ecology at the extremes of species' ranges. *Environ. Rev.* **18**, 1–20 (2010).
113. J. G. Sørensen, J. Dahlgaard, V. Loeschcke, Genetic variation in thermal tolerance among natural populations of Drosophila buzzatii: Down regulation of Hsp70 expression and variation in heat stress resistance traits. *Funct. Ecol.* **15**, 289–296 (2001).
114. K. A. Mitchell, C. M. Sgrò, A. A. Hoffmann, Phenotypic plasticity in upper thermal limits is weakly related to Drosophila species distributions: Plasticity is weakly related to Drosophila distributions. *Funct. Ecol.* **25**, 661–670 (2011).
115. B. van Heerwaarden, V. Kellermann, C. M. Sgrò, Limited scope for plasticity to increase upper thermal limits. *Funct. Ecol.* **30**, 1947–1956 (2016).
116. L. B. Jørgensen, H. Malte, J. Overgaard, How to assess Drosophila heat tolerance: Unifying static and dynamic tolerance assays to predict heat distribution limits. *Funct. Ecol.* **33**, 629–642 (2019).
117. M. Carlassara *et al.*, Population-specific responses to developmental temperature in the arboviral vector Aedes albopictus: Implications for climate change. *Glob. Change Biol.* **30**, e17226 (2024).
118. L. L. Robert, J. K. Olson, Effects of sublethal dosages of insecticides on Culex quinquefasciatus. *J. Am. Mosq. Control Assoc.* **5**, 239–246 (1989).
119. B. Ameneshewa, M. W. Service, The relationship between female body size and survival rate of the malaria vector Anopheles arabiensis in Ethiopia. *Med. Vet. Entomol.* **10**, 170–172 (1996).
120. E. O. Lyimo, W. Takken, Effects of adult body size on fecundity and the pre-gravid rate of Anopheles gambiae females in Tanzania. *Med. Vet. Entomol.* **7**, 328–332 (1993).
121. R. S. Nasci, Relationship of wing length to adult dry weight in several mosquito species (Diptera: Culicidae). *J. Med. Entomol.* **27**, 716–719 (1990).
122. E. Van Handel, J. F. Day, Correlation between wing length and protein content of mosquitoes. *J. Am. Mosq. Control Assoc.* **5**, 180–182 (1989).
123. M. D. Abramoff, P. J. Magalhães, S. J. Ram, Image processing with ImageJ. *Biophotonics Int.* **11**, 36–42 (2004).
124. D. L. Huestis *et al.*, Variation in metabolic rate of Anopheles gambiae and A. arabiensis in a Sahelian village. *J. Exp. Biol.* **214**, 2345–2353 (2011).
125. P. A. Ross, N. M. Endersby, H. L. Yeap, A. A. Hoffmann, Larval competition extends developmental time and decreases adult size of wMelPop Wolbachia-infected Aedes aegypti. *Am. J. Trop. Med. Hyg.* **91**, 198–205 (2014).
126. D. Bates, M. Maechler, B. Bolker, S. Walker, lme4: Linear mixed-effects models using Eigen and S4 (2014). Deposited 23 June 2014.
127. H. Cheng, G. T. Concepcion, X. Feng, H. Zhang, H. Li, Haplotype-resolved de novo assembly using phased assembly graphs with hifiasm. *Nat Methods* **18**, 170–175 (2021).
128. J. H. Boyle *et al.*, A linkage-based genome assembly for the mosquito Aedes albopictus and identification of chromosomal regions affecting diapause. *Insects* **12**, 167 (2021).
129. C. Peng *et al.*, A draft genome assembly of Culex pipiens pallens (Diptera: Culicidae) using PacBio sequencing. *Genome Biol. Evol.* **13**, evab005 (2021).
130. J. Soghigian, T. G. Andreadis, T. P. Livdahl, From ground pools to treeholes: Convergent evolution of habitat and phenotype in Aedes mosquitoes. *BMC Evol. Biol.* **17**, 262 (2017).
131. M. Alonge *et al.*, Automated assembly scaffolding using RagTag elevates a new tomato system for high-throughput genome editing. *Genome Biol.* **23**, 258 (2022).
132. J. M. Flynn *et al.*, RepeatModeler2 for automated genomic discovery of transposable element families. *Proc. Natl. Acad. Sci. U.S.A.* **117**, 9451–9457 (2020).
133. A. Smit, R. Hubley, P. Green, RepeatMasker2 (2021). Deposited 1 April 2021.
134. A. Lomsadze, V. Ter-Hovhannisyan, Y. O. Chernoff, M. Borodovsky, Gene identification in novel eukaryotic genomes by self-training algorithm. *Nucleic Acids Res.* **33**, 6494–6506 (2005).
135. M. Stanke, M. Diekhans, R. Baertsch, D. Haussler, Using native and syntenically mapped cDNA alignments to improve de novo gene finding. *Bioinformatics* **24**, 637–644 (2008).
136. T. Brůna, K. J. Hoff, A. Lomsadze, M. Stanke, M. Borodovsky, BRAKER2: Automatic eukaryotic genome annotation with GeneMark-EP+ and AUGUSTUS supported by a protein database *NAR Genomics Bioinform.* **3**, lqaa108 (2021).
137. A. M. Bolger, M. Lohse, B. Usadel, Trimmomatic: A flexible read trimming tool for Illumina NGS data (2014). Deposited 1 April 2014.
138. H. Li, Aligning sequence reads, clone sequences and assembly contigs with BWA-MEM (2013). Deposited 26 May 2013.
139. P. Danecek *et al.*, Twelve years of SAMtools and BCFtools. *GigaScience* **10**, giab008 (2021).
140. P. Danecek *et al.*, The variant call format and VCFtools. *Bioinformatics* **27**, 2156–2158 (2011).
141. B. R. Evans *et al.*, A multipurpose, high-throughput single-nucleotide polymorphism chip for the dengue and yellow fever mosquito, Aedes aegypti. *G3 (Bethesda)* **5**, 711–718 (2015).
142. S. Purcell *et al.*, PLINK: A tool set for whole-genome association and population-based linkage analyses. *Am. J. Hum. Genet.* **81**, 559–575 (2007).
143. C. C. Chang *et al.*, Second-generation PLINK: Rising to the challenge of larger and richer datasets. *GigaScience* **4**, 7 (2015).
144. S. Soudi *et al.*, Genomic signatures of local adaptation in recent invasive Aedes aegypti populations in California. *BMC Genomics* **24**, 311 (2023).
145. B. S. Weir, C. C. Cockerham, Estimating F-statistics for the analysis of population structure. *Evolution* **38**, 1358–1370 (1984).
146. M. C. Whitlock, K. E. Lotterhos, Reliable detection of loci responsible for local adaptation: Inference of a null model through trimming the distribution of FST. *Am. Nat.* **186**, S24–S36 (2015).
147. J. P. Andersen, A. Schwartz, J. B. Gramsbergen, V. Loeschcke, Dopamine levels in the mosquito Aedes aegypti during adult development, following blood feeding and in response to heat stress. *J. Insect Physiol.* **52**, 1163–1170 (2006).
148. D. L. Cameron *et al.*, GRIDSS2: Comprehensive characterisation of somatic structural variation using single breakend variants and structural variant phasing. *Genome Biol.* **22**, 202 (2021).
149. X. Chen *et al.*, Manta: Rapid detection of structural variants and indels for germline and cancer sequencing applications. *Bioinformatics* **32**, 1220–1222 (2016).
150. R. M. Layer, C. Chiang, A. R. Quinlan, I. M. Hall, LUMPY: A probabilistic framework for structural variant discovery. *Genome Biol.* **15**, R84 (2014).
151. T. Rausch *et al.*, DELLY: Structural variant discovery by integrated paired-end and split-read analysis. *Bioinformatics* **28**, i333–i339 (2012).
152. M. Kirsche *et al.*, Jasmine and Iris: Population-scale structural variant comparison and analysis. *Nat. Methods* **20**, 408–417 (2023).
153. M. Mahmoud *et al.*, Structural variant calling: The long and the short of it. *Genome Biol.* **20**, 246 (2019).
154. S. M. Rudman *et al.*, Direct observation of adaptive tracking on ecological time scales in Drosophila. *Science* **375**, eabj7484 (2022).
155. G. Bell, A. Gonzalez, Evolutionary rescue can prevent extinction following environmental change. *Ecol. Lett.* **12**, 942–953 (2009).
156. R. Gomulkiewicz, R. G. Shaw, Evolutionary rescue beyond the models. *Philos. Trans. R. Soc. B* **368** (2013).
157. A. Gonzalez, O. Ronce, R. Ferriere, M. E. Hochberg, Evolutionary rescue: An emerging focus at the intersection between ecology and evolution. *Philos. Trans. R. Soc. B* **368**, 20120404 (2013).
158. S. M. Carlson, C. J. Cunningham, P. A. H. Westley, Evolutionary rescue in a changing world. *Trends Ecol. Evol.* **29**, 521–530 (2014).
159. P. Gienapp *et al.*, Predicting demographically sustainable rates of adaptation: Can great tit breeding time keep pace with climate change? *Philos. Trans. R. Soc. B* **368**, 20120289 (2013).
160. A. Bush *et al.*, Incorporating evolutionary adaptation in species distribution modelling reduces projected vulnerability to climate change. *Ecol. Lett.* **19**, 1468–1478 (2016).
161. O. Cotto *et al.*, A dynamic eco-evolutionary model predicts slow response of alpine plants to climate warming. *Nat. Commun.* **8** (2017).
162. J. A. F. Diniz-Filho *et al.*, A macroecological approach to evolutionary rescue and adaptation to climate change. *Ecography* **42**, 1124–1141 (2019).
163. P. J. Huxley, K. A. Murray, S. Pawar, L. J. Cator, The effect of resource limitation on the temperature dependence of mosquito population fitness. *Proc. R. Soc. B* **288**, 20203217 (2021).
164. P. J. Huxley, K. A. Murray, S. Pawar, L. J. Cator, Competition and resource depletion shape the thermal response of population fitness in Aedes aegypti. *Commun. Biol.* **5**, 1–11 (2022).
165. C. R. Linnen, H. E. Hoekstra, Measuring natural selection on genotypes and phenotypes in the wild. *Cold Spring Harb. Symp. Quant. Biol.* **74**, 155–168 (2009).
166. J. Yang, S. H. Lee, M. E. Goddard, P. M. Visscher, GCTA: A tool for genome-wide complex trait analysis. *Am. J. Hum. Genet.* **88**, 76–82 (2011).
167. A. Forde, G. Hemani, J. Ferguson, Review and further developments in statistical corrections for Winner's Curse in genetic association studies. *PLoS Genet.* **19**, e1010546 (2023).
168. L. I. Couper *et al.*, Mosquito thermal selection. GitHub. https://github.com/lcouper/MosquitoThermalSelection. Deposited 28 April 2022.